FLUCTUATIONS OF STEP EDGES: REVELATIONS ABOUT ATOMIC PROCESSES UNDERLYING SURFACE MASS TRANSPORT

T. L. EINSTEIN*, S. V. KHARE,*,** O. PIERRE-LOUIS*
*Department of Physics, University of Maryland, College Park, MD 20742-4111,
einstein@surface.umd.edu, opl@surface.umd.edu
**Present address: Department of Physics, Ohio State University, Columbus, OH 43210,
khare@campbell.mps.ohio-state.edu

ABSTRACT

Experimental advances in recent years make possible quantitative observations of step-edge fluctuations. By applying a capillary-wave analysis to these fluctuations, one can extract characteristic times, from which one learns about the mass-transport mechanisms that underlie the motion as well as the associated kinetic coefficients [1-3]. The latter do not require *a priori* insight about the microscopic energy barriers and can be applied to situations away from equilibrium. We have studied a large number of limiting cases and, by means of a unified formalism, the crossover between many of these cases[4]. Monte Carlo simulations have been used to corroborate these ideas. We have considered both isolated steps and vicinal surfaces; illustrations will be drawn from noble-metal systems, though semiconductors have also been studied. Attachment asymmetries associated with Ehrlich-Schwoebel barriers play a role in this behavior. We have adapted the formalism for nearly straight steps to nearly circular steps in order to describe the Brownian motion of single-layer clusters of adatoms or vacancies on metal surfaces, again in concert with active experimental activity [3,5]. We are investigating the role of external influences, particularly electromigration, on the fluctuations.

INTRODUCTION

In addition to providing information about the energy of kinks, thermal fluctuations of steps on a vicinal surface provide a rich source of insight into the microscopic atomic processes which underlie the fluctuations. In recent years it has become possible to make quantitative measurements of these fluctuations using STM (scanning tunneling microscopy), LEEM (low-energy electron microscopy), and REM (reflection electron microscopy). The fluctuations of the steps can be viewed as a form of Brownian motion and can be analyzed using a capillary-wave approach and Langevin formalism. From this analysis one can deduce the key macroscopic parameters—step stiffness, step-step interaction strength, and transport coefficient—which govern the macroscopic behavior of the steps. These parameters can then be applied to situations out of equilibrium or in which the steps are driven by external forces. Furthermore, the analysis of nearly-straight steps can be adapted to treat nearly-circular steps and thereby describe the Brownian motion of monolayer clusters of atoms or vacancies on surfaces, for which quantitative experimental data has also been obtained over the last few years.

This submission has its roots in a conference review paper [3] but emphasizes new results only briefly broached there. Our scientific purposes are 1) to summarize the assumptions and results of the unified formalism and an alternative formalism [4]; 2) to review the application of this formalism to the diffusion of single-layer clusters, using the notation of Ref. [4]; 3) to discuss the results in view of recent experiments and theory; and 4) to briefly describe work in progress to consider electromigration in this framework.

Mat. Res. Soc. Symp. Proc. Vol. 528 © 1998 Materials Research Society

EQUILIBRIUM FLUCTUATIONS OF ISOLATED STRAIGHT STEPS

In Monte Carlo simulations of the SOS model or similar lattice systems, one can graphically watch how the step configuration changes as adatoms or vacancies attach to or detach from the step edge [4]. In LEEM, REM, or STM experiments, one either lacks the resolution to observe atomic events or these events happen so rapidly that they cannot be observed individually. The challenge, then, is to deduce as much as possible about these atomic processes from observations of the step configurations alone. To do so, we apply capillary wave analysis. In what has been called "Maryland" notation, the steps are taken to run along the *y* direction, so that excursions perpendicular to it are in the *x* direction. Thus, the position of the n^{th} step, relative to a uniform staircase, is denoted $x_n(y,t)$. A motivation for this notation is that formulas can be easily compared to the one-dimensional limit by removing the y dependence. As the "wavelengths" (characteristic size in $\hat{\mathbf{y}}$) of the equilibrium fluctuations increase, so do their amplitudes (in $\hat{\mathbf{x}}$) and their duration, as shown below.

It has long been known [6] that there are three well-characterized limiting cases, denoted hereafter EC, TD, and PD [2,7], depending on what process limits the rate at which fluctuations heal. In EC [2D] evaporation/condensation, or attachment/ detachment, of atoms and/or vacancies at the step edge limit the production and decay of fluctuations. Once the adatom or vacancy is free of the step, it is assumed to be instantly equilibrated into a 2D "gas" of mass "carriers" on the terraces. In TD, diffusion across the terrace is the rate-limiting process, leading to a non-uniform distribution of carriers on the terrace that decays exponentially toward the thermal value for a flat surface. In PD (periphery (or edge) diffusion), motion along the step edge limits the rate of the healing of fluctuations.

To make quantitative progress, we use a Langevin formulation. This amounts to an overdamped harmonic oscillator driven by a noise term [8]. We have described this process several times before.[2–4,9]. It is very helpful to perform a Fourier transform along the mean direction of the step, i.e. writing x(y,t) as $\Sigma_q \exp(iqy)x_q(t)$ in this capillary-wave analysis. It is particularly fruitful to study the behavior of the (measurable!) [10–12] autocorrelation function $G_q(t-t')$ of the capillary modes:

$$G_q(t-t') \equiv \left\langle \left| x_q(t) - x_q(t') \right|^2 \right\rangle = 2\left\langle \left| x_q(t) \right|^2 \right\rangle - 2\left\langle x_q(t) x_q(t') \right\rangle = A\left(1 - e^{-|t-t'|/\tau_q}\right) \qquad (1)$$

From equipartition arguments, one finds that the prefactor $A = 2k_BT/\tilde{\beta}q^2L_y$ [where L_y is the size of the system along $\hat{\mathbf{y}}$] depends simply on known quantities, except perhaps the step stiffness $\tilde{\beta}$, which can thus be determined from this relation or checked with previous independent determinations. [The stiffness is the coefficient of the integral of $(1/2)(\partial x/\partial y)^2$ in the Hamiltonian of the step; $\tilde{\beta}(\theta) = \beta(\theta) + \beta''(\theta)$, where $\beta(\theta)$ is the free energy per length of a step.] The q^2 dependence does not depend on the limiting case. On the other hand, by integrating eqn. (2) and computing $\langle x_q(t)\, x_Q(t')\rangle$, we find

$$\tau_q^{-1} = (\Omega\tilde{\beta} / k_BT)q^2\tilde{f}(q); \qquad \tilde{f}(q) = k_+ + k_-,\ 2D_{su}|q|,\ 2a_\perp D_{st}q^2 \qquad (2)$$

for the cases EC, TD, and PD, respectively. This notation generally follows that adopted in Ref. [4] in an attempt to reduce confusion about physical interpretation. (The connection between this notation and others is described in Appendix D of ref. [4]. The quantity $\tilde{f}$ is $L_yf_q/2$ of ref. [4], where f_q is the weighting factor in the orthogonality condition for the Langevin noise associated with $x_q(t)$.) The subscripts su and st are abbreviations for surface and step, respectively. The

lattice spacings $a_\perp$ and $a_\parallel$ are in the unit spacings in the $\hat{x}$ and the $\hat{y}$ directions, respectively, and $\Omega = a_\perp a_\parallel$ is the area per atom (i.e. of the surface unit cell). The writing of eqn. (2) anticipates the definition of a reduced stiffness $S \equiv \Omega\tilde{\beta}/k_BT$, with dimensions of length. Thus, $\tilde{f}$ has the dimensions of velocity. In our standard linear kinetic approximation, the coefficients $k_{-(+)}$ are the proportionality constants relating the difference—normalized by the Boltzmann energy—of the chemical at the upper (lower) edge of the step and the chemical potential of the step itself to the step-edge velocity $\dot{x}(y,t)|_{-(+)}$. The factors of 2 reflect the simplifying assumption that these are the same on both sides of the step edge. The three macroscopic transport coefficients can be re-expressed in terms of characteristic inverse times for attachment/detachment, hopping along the terrace, and hopping along the step edge, respectively. These characteristic times can be computed straightforwardly in simple models. However, in interpreting complicated systems such as found in most experiments, they are better viewed as effective parameters that involve an average over several microscopic times. The driving philosophy is that these same average times will be involved in all kinetic processes not far from equilibrium, so that it is counterproductive to try to extract microscopic parameters from one measurement and reconstruct macroscopic parameters to interpret a different experiment.

The behavior $\tau_q^{-1} \propto q^2$ in EC arises because the relaxation is proportional to the change in the chemical potential from its equilibrium value μ_s, which in this case is just proportional to the local curvature of the step edge. The extra factor of q^2 in PD ($\tau_q^{-1} \propto q^4$) arises from the additional $-\partial^2/\partial y^2$ coming from the conservation condition. The extra factor of $|q|$ ($\tau_q^{-1} \propto |q|^3$) in TD comes from the exponential decay of the concentration toward the terrace value as one moves away from the step edge. In contrast, the terrace concentration is uniform in EC and effectively zero in PD. Notice from eqn. (1) that in all three cases the early-time behavior of $G_q(t)$ is linear in t, characteristic of diffusive, exponential relaxation. In contrast, the real space analogue, the mean-square width $w^2(t-t') = \langle|x(t) - x(t')|^2\rangle$ is not linear in any of the simple cases; instead, $w^2(t) \propto t^{1/2}$, $t^{1/3}$, $t^{1/4}$, for EC, TD, PD, respectively. Fluctuations of positions along the step edge—in contrast to those of the q-modes—are interdependent.

There are other ways to obtain many of these results. Decades ago Mullins [6] showed the fruitfulness of formulating the problem in terms of a step chemical potential. Bales and Zangwill [13] used the linear kinetic approximation that the step velocity is proportional to the difference between the adatom concentration near the step edge and its equilibrium value. Pimpinelli *et al.* [14] trisect each system into a fluctuating step, a reservoir of atoms enabling the fluctuations, and a pipe connecting the two, through which the exchange of atoms occurs. From this incisive perspective, they can quickly account for a large number of limiting cases, including multi-step situations, but sacrifice the factors of π and the like appearing in more precise derivations. B. Blagojević and P.M. Duxbury [15] formulate the problem in terms of the probability P(y) that atoms leaving the step at one point return to this step a distance y away. Not only do they retrieve the early-time growth of the mean-square width in the three limiting cases EC, TD, and PD, but they can achieve intermediate values $t^{1/(\alpha+1)}$ if $P(y) \propto y^{-\alpha}$. It is not immediately clear how this particular form of P(y) relates to the physical nature in our formulation. We [4,5] have also studied cross-over behavior between limiting cases by considering a unified formulation that considers all three mechanisms simultaneously, as well as reproducing and extending the multistep behavior of Pimpinelli *et al.* [14].

As an illustration of the application to actual data of the analysis procedure developed at Maryland, we consider the case of an isolated step on Ag(110) directed 30° from the close-packed $[1\bar{1}0]$ direction, measured by STM at room temperature by Reutt-Robey's group at Maryland [12, 16, 17]. A best fit of the early-time measurements of the autocorrelation function is $w^2(t) = 33.7\text{Å}^2 \cdot t^{0.49}$, consistent with EC. In the capillary wave analysis, the lowest value of q was 2.1 ×

10^{-3} Å^{-1}, corresponding to a wavelength 3000Å. Some half-dozen values of q up to eight times that lowest value were analyzed for up to 1000 sec. From the fits of $G_q(t)$, A (and thence $\tilde{\beta} \approx 18$ meV/Å) and τ_q were obtained. In the plot of τ_q^{-1} vs. q, the fit to q^2 was much better than the alternatives, supporting the view that the fluctuations are EC limited. From the prefactor of this fit and the deduced $\tilde{\beta}$, we estimate the time between atomic attachment/detachment events $\tau_a \approx 350$ msec. For an isolated step along the [1$\bar{1}$0] direction, the stiffness is over 8 times as large, but $\tau_a \approx$ 400 msec, indicating that the ability of steps to supply Ag atoms to the terrace ($\tau_a^{-1} \approx 3$ [events] per second [per step site]) has little dependence on step orientation (and so kink density) [12]. For Si surfaces at much higher temperatures, also examples of $\tau_q^{-1} \propto q^2$, the mobilities are much higher: for Si (111) at 900°C, $\tau_a^{-1} \approx 10^6$ atoms/sec [13, 18]; for Si (100) at 700–1200°C, $\tau_a^{-1} \approx 10^3 - 10^6$ dimers/sec [11, 19]. Kuipers *et al.* [20,21] had found similar fluctuations on vicinal Au(110) and Pb(111). Cases of vicinals on which fluctuations with $\tau_q^{-1} \propto q^4$ have been observed are: Ag(111) [22], Cu(100) [22–26], Ag(100) [27, 28], and Pt (111) [29]. To date there have been no observations of $\tau_q^{-1} \propto |q|^3$; as discussed in the next section, there may be reasons for this related to the isolated-step approximation. It can, however, be readily seen in Monte Carlo simulations of the SOS model [2].

CROSSOVER BEHAVIOR OF VICINAL SURFACES

The preceding approach relies on a different Langevin equation, each with its distinct restoring force, for each of the three cases of isolated steps. We have since developed a more general formalism that takes into account all three mechanisms in a unified way, thereby allowing us to assess in a systematic way the extents of the various limiting regimes and the nature of the crossover between them.

As indicated above in conjunction with the definition of $k_\pm$, we begin by assuming that the contribution to the step velocity on either side of the step edge is linearly proportional to the change in the chemical potential on that side of the edge from the equilibrium value μ_s of the step edge. In the limit of small deviations ($|x'(y)| \ll 1$), μ_s reduces to $-\tilde{\beta}\Omega x''$. While in principle the chemical potential should be a function of both spatial coordinates and the time, as in the classical Stefan problem, we make the usual quasistatic approximation of neglecting any explicit time dependence of it. (In studies of the analogous growth problem, this approximation was shown to be reasonable until the deposition flux became so large that nucleation of islands began on the terraces [30]. Then our problem reduces to solving Laplace's equation for $\mu(x,y)$. [Equivalently, we could work in terms of the concentration field c(x,y); this involves no extra effort if we make the lowest order approximation $\mu(x,y)/k_BT = (c(x,y)/c_{su}) - 1$, where c_{su} is the equilibrium concentration of the "carriers" far from the step. To include mass conservation, we stipulate that the step velocity can be produced either by carriers by atoms diffusing along the step edge or by carriers traveling between the terrace and the step (so proportional to D and to the normal current, viz. the normal gradient of μ). Combining this boundary condition with the linear kinetic assumption (and dividing out the Boltzmann energy) leads to the important equation

$$a_\perp D_{st} \frac{\partial^2 \mu(0^\pm, y)}{\partial y^2} \mp D_{su} \frac{\partial \mu(0^\pm, y)}{\partial x} = k_\pm \left\{ \mu(0^\pm, y) - \mu_s \right\} = k_B T \dot{x}(y,t)\big|_\pm \qquad (3)$$

This formulation contains the standard and arguably unphysical implicit approximation that the energy barrier for an atom to attach to the step (presumably onto a kink site) from the terrace is the same as that to attach from a mobile state along the step edge onto a kink. (More precisely, the implicit assumption is that these rates are comparable, but it is hard to imagine that the prefactors

would just compensate for the differences in the Boltzmann factors.) We discuss below how to generalize the conventional perspective embodied in eqn. (3) to take into account the different possible rates.

It is again fruitful to perform a capillary-wave analysis, Fourier transforming along $\hat{y}$ and thereby introducing the wavevector q. The dimensionless parameters of the problem then become apparent:

$$a_q^{\pm} \equiv D_{su}|q| / k_{\pm}; \quad b_q^{\pm} \equiv D_{st} a_{\perp} q^2 / k_{\pm}; \quad |q|\ell; \quad r \equiv k_- / k_+ \tag{4}$$

Here $a_q^{\pm}$ and $b_q^{\pm}$ are dimensionless measures of the terrace diffusion and the step-edge diffusion relative to the attachment/detachment rate, respectively. Many [30–32] use the so-called "kinetic length" $d_{\pm} \equiv D_{su}/k_{\pm}$ instead of $a_q^{\pm}$. Anticipating the next section discussing vicinal surfaces, the product $q\ell$ measures the ratio of the mean terrace width ℓ to the wavelength of the fluctuation of the step edge.

As for the limiting cases, we probe the dynamics by computing the inverse time constant associated with the wavevector-dependent decay of fluctuations:

$$\frac{1}{\tau_q} = \frac{1}{\tau_q^+} + \frac{1}{\tau_q^-}; \qquad \frac{1}{\tau_q^{\pm}} \equiv S k_{\pm} q^2 \left(\frac{a_q^{\pm} + b_q^{\pm}}{1 + a_q^{\pm} + b_q^{\pm}} \right) \tag{5}$$

To describe the crossover behavior, we compute an effective dynamic exponent z_q defined by

$$z_q = -\partial \log \tau_q / \partial \log |q| \tag{6}$$

For an isolated step we define for convenience $p_q \equiv a_q + b_q$ and allow motion on only the lower side of the step. Then we find

$$z_q = 2 + \left[\frac{p_q + b_q}{p_q(1+p_q)} \right] \left[1 - \frac{r(1-r)p_q(1+p_q)}{(p_q + r)(p_q + p_q r + 2r)} \right]. \tag{7}$$

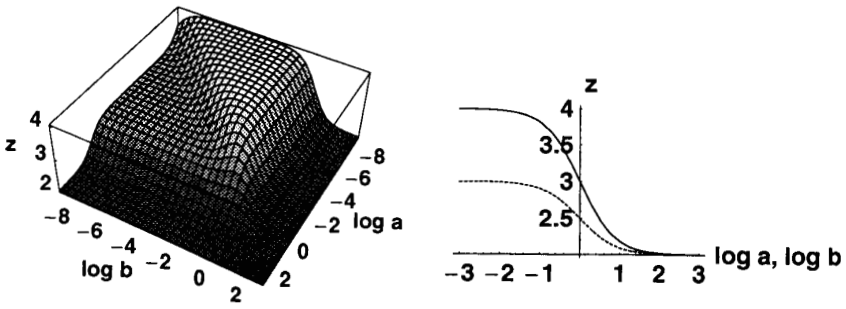

Fig. 1. a) 3D replot of the contour plot (Fig. 2 of ref. [4]) of the effective exponent z_q as a function of the common logarithms of the dimensionless ratios a_q and b_q for isolated steps ($\ell = \infty$) and b) simple plots of z_q vs. log b_q—solid line (or log a_q—dashed line) when $a_q = 0$ (or $b_q = 0$, respectively). Note that z_q can take on values below 4, even down to 2, when motion is confined to the step edge ($a_q = 0$).

Written in this way, it is obvious that the expression in the right-most bracket of eqn. (7) becomes one at both r=1 *and* r=0, i.e. full symmetry or asymmetry. In either of these cases, we display in Fig.1 a three-dimensional plot of z_q vs. a_q and b_q. We see that for most of phase space we are on plateaux of $z_q = 2, 3, 4$, corresponding to EC, TD, and PD, respectively, or cases **B**, **C** and **F** in the notation of Pimipinelli *et al.* [14]. Only in fairly narrow regimes slightly over an order of magnitude wide are there non integer exponents. We see that for large values of a_q and b_q, corresponding to small values of k that limit transport, we recover EC. Likewise, when D_{su} or D_{st} are the limiting quantities (so $b_q \ll a_q \ll 1$ and $a_q \ll b_q \ll 1$), we recover TD or PD, respectively. To emphasize this point, we plot in Fig. 1b the value of z_q when either a_q or b_q vanish.

The crossover regions are rather well confined and smooth, so that if one measures the effective exponent over a decade or so, it should have a well-defined value (i.e., the log-log plot should be linear) only if one is in one of the plateau regions. Conversely, if one finds an effective exponent other than 2, 3, or 4, the fits should not be good, and there should be indications of monotonic variation. With two or more decades of data, one reaches one of the three integer plateau regions. *We emphasize that these statements assume that the data is plotted in terms of one of the dimensionless ratios of eqn. (4); conversion from measurable variables may not always be simple.* If any of these statements are inconsistent with the data, then either the experiment is flawed or the theory has left out some crucial ingredient of the system.

The behavior of the expression in the right-most bracket in eqn. (7) has been thoroughly characterized in ref. [4]. For positive p_q, it has a smooth minimum of ~0.83 near $r \approx 0.4$. At smaller p_q the minimum occurs at smaller values of r. Overall, the factor appears most significant for positive values of a_q and b_q, regions in which $z_q \approx 2$ (EC plateau), so that the r-independent factor is tiny.

To generalize from an isolated step to a vicinal surface, we must consider the fluctuations $x_n(y,t)$ of each step from its equilibrium position and associate an independent chemical potential with each terrace as well as another (μ_{sn}) with each step. Then there is a separate mass-conservation boundary condition equivalent to eqn. (3) for each side of each step. To solve the resulting set of coupled equations, one can Fourier transform in the $\hat{x}$ direction [31,33]. However, for present purposes we just consider the acoustic or in-phase combination $x_\Sigma(y,t)$ and the optical or out-of-phase combination $x_\Delta(y,t) \equiv \Sigma (-1)^n x_n(y,t)$. We have worked out a large number of limiting cases, as given in Table 1 of ref. [4].

To consider the crossover between cases **B**, **C**, **D**, and **E**, we focus on the dynamic exponent associated with $x_{\Delta,q}(t)$, where we expect interstep effects to be maximal. To simplify the algebra by setting $D_{st} = 0$, since diffusion along the step edge essentially affects each step independently, at least for small amplitudes. Even then, the resulting expression for z_q, given in ref. [4], is rather formidable. In the limit $|q|\ell \to \infty$, the expression does reduce to EC or TD (cases B or C).

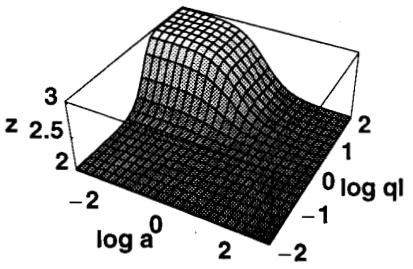

Fig. 2. 3D replot of the contour plot (Fig. 4) of ref. [4] of the effective exponent z_q as a function of the common logarithms of the dimensionless ratios a_q and $|q|\ell$ for $b_q = 0$ and no Ehrlich-Schwoebel barrier.

In Fig. 2 we present a 3-d plot of the effective dynamic exponent as a function of a_q and $|q|\ell$. For $a_q \ll 1$ and $|q|\ell \gg 1$, we see a plateau corresponding to case **C**. However, for $|q|\ell \ll 1$, a plateau at $z_q = 3$, corresponding to the TD behavior of case **C**. There is a smooth descent to $z_q = 2$, characteristic of EC, in the other three quadrants. The crossover occurs over roughly a decade along either axis. The two quadrants with $a_q \gg 1$ correspond to case B, while the remaining quadrant with $a_q \ll 1$ and $|q|\ell \ll 1$ is case **D**, in which the long-wavelength TD fluctuations on a step relatively close to its neighbors have the signature of EC fluctuations because a power of $|q|$ is supplanted by $1/\ell$. The general behavior seen in Fig. 2 holds till remarkably small r. Qualitatively, the descent from the plateau occurs at decreasing values of a_q and ripple develops on the lower plateau along the diagonal $a_q|q|\ell \approx 1$. For r = 1/2, this ripple at its largest corresponds to $z_q \approx 2.05$. By r=0.1, this ripple has increased to $z_q \approx 2.5$. (See Fig. 3a.) Only for very small r does qualitatively new behavior occur. The ripple broadens and grows, and its center shifts to smaller values of a_q as r decreases. By $r \approx 10^{-5} - 10^{-6}$, a plateau at $z_q = 4$ has formed in the quadrant $a_q \ll 1$ and $|q|\ell \ll 1$. (See Fig. 3b.) This region corresponds to case **E**. For r=0, $a_q \ll 1$, we can show $z_q = 4$ analytically. (Interested readers should refer to eqn. (53 of ref. [4].) Such behavior evidently will occur only for extremely small r, with virtually no attachment to steps from their upper side.

Bonzel and Mullins [34] have carried out a similar analysis for an isolated straight step, and we [4, 35] have extended our formalism to treat both such steps and a vicinal surface, i.e. an infinite array of steps. We have also investigated an alternative, physically more plausible formalism, as described briefly below and expounded in Appendix A of ref. [4]. As for islands, one can examine the crossover between the three limiting regimes for isolated steps. The main result, again, is that the crossover regions comprise a rather narrow portion of phase space. We also recover the important cases of transport between steps when the q-dependence of τ_q^{-1} and the early-time dependence of the mean-square width do not correspond to the corresponding behavior of an isolated step, cases D and E in Pimpinelli *et al.* [14]. In case D, there is no diffusion along the step edge ($D_{st} = 0$). Since $D_{su}|q|/k_{\pm} \ll 1$, the transport is terrace-diffusion limited, but now $|q|\ell \ll 1$. As a result, $w^2 \sim t^{1/2}$ and $\tau_q^{-1} \propto \ell^{-1}q^2$: the latter inequality leads to a factor of q being replaced by ℓ^{-1}. For case E, atomic motion along the step edge is again forbidden, $D_{su}|q|/k_{\pm} \ll 1$, and $|q|\ell \ll 1$, but now there is also the condition of a perfect (infinite) Schwoebel barrier: atoms approaching a step from the upper side are reflected back rather than crossing over the step and possibly attaching to it. Following through the algebraic reductions from taking the appropriate formal limits, we find that $\tau_q^{-1} \propto \ell\, q^4$ rather than $|q|^3$, and $w^2 \sim t^{1/4}$. Thus, it is important to measure step fluctuations for different vicinalities to be certain of the correct assignment of transport mode. On the other hand, if one does find $|q|^3$ or $t^{1/3}$ behavior, it most likely is due to the TD mechanism.

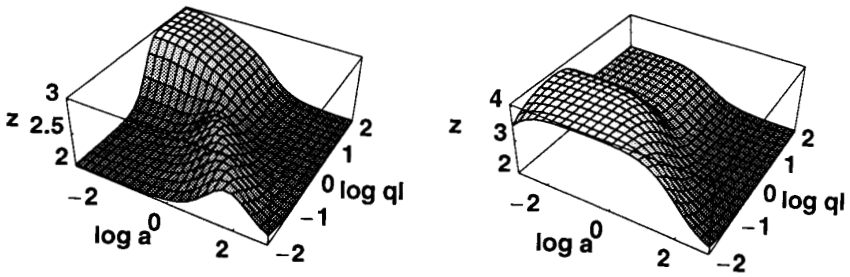

Fig. 3. 3D plots of the effective exponent z_q as a function of the common logarithms of the dimensionless ratios a_q and $|q|\ell$ for $b_q = 0$ and a) $r = 10^{-1}$; b) $r = 10^{-6}$ (replot of Fig. 5b of ref. [4]).

Other crossover behavior can arise when one moves to a regime where the continuum picture is not valid. For examples, Giesen-Seibert *et al.* [25] show that for PD, at very early times w^2 behaves like $t^{1/2}$ rather than $t^{1/4}$ because the dynamics are dominated by random walks of kinks. In their simulations the effective exponent decreases smoothly with increasing temperature, with no evident crossover in any of the fixed–T log–log plots of w^2 vs. t. They also show how to take into account "fast events," viz. rapid, inconsequential back-and-forth motion of atoms ("blinkers"). This work builds on an earlier analysis [24] in which they examine the structure of the probability distribution of the time between jumps as a function of the number of scans and the time of each scan, showing that the result does not depend simply on the product of these two arguments and that this sort of analysis can be used to filter out blinker events. Masson *et al.* [26a] propose a way to scale the step-step correlation function in terms of the STM scanning speed to allow the separation of diffusive behavior at fast scanning speeds from rapid temporal fluctuations at slow speeds.

ALTERNATIVE FORMALISM FOR STEPS

As noted above, the use of a single kinetic coefficient for both terrace and edge motion, while convenient, is open to question. For example, in very recent LDA/GGA on Al (111), Bogicevic *et al.* [36] found the detachment barrier for hopping from a kink position to a step edge to be about 1/2 eV (somewhat more for a B step, with (111) microfacet, but an exchange process also has a barrier around 1/2 eV); in contrast, the barrier for detachment from an edge to the terrace is about 0.8 eV, so that this process becomes activated at about twice the temperature of the former.

To account for this difference, we [4] can consider separate kinetic coefficients $k_\pm^{su}$ and $k_\pm^{st}$ for surface (terrace) and step-edge processes. Then we must generalize eqn. (3) to

$$a_\perp D_{st}\frac{\partial^2\mu(0^\pm,y)}{\partial y^2}=k_\pm^{st}\left\{\mu(0^\pm,y)-\mu_s\right\};\qquad \mp D_{su}\frac{\partial\mu(0^\pm,y)}{\partial x}=k_\pm^{su}\left\{\mu(0^\pm,y)-\mu_s\right\} \tag{8}$$

We then redefine our dimensionless ratios and find a new expression for the inverse time constant

$$a_q'^{\pm}\equiv D_{su}|q|/k_\pm^{su}\qquad b_q'^{\pm}\equiv D_{st}a_\perp q^2/k_\pm^{st}\qquad \frac{1}{\tau_q^\pm}\equiv Sq^2\left(\frac{k_\pm^{su}a_q'^{\pm}}{1+a_q'^{\pm}}+\frac{k_\pm^{st}b_q'^{\pm}}{1+b_q'^{\pm}}\right) \tag{9}$$

We emphasize that this is not merely an extension of the previous formalism: if we take the limit $k_\pm^{su}=k_\pm^{st}=k_\pm$, we do not retrieve the previous inverse time constant of eqn. (5). The various limits in the table of ref. [4] remain unchanged provided we make the appropriate substitution for $k_\pm$. While Fig. 1 will change, the others will remain unaffected once $k_\pm^{su}$ replaces $k_\pm$ and $a'^{\pm}_q$ replaces $a_q^\pm$.

APPLICATIONS TO DIFFUSION OF LARGE SINGLE-LAYER CLUSTERS

As discussed in several papers earlier in this proceedings, and elsewhere as well, the diffusion of large single-layer clusters of [100's to 1000's of] atoms or vacancies can now be measured quantitatively with STM. Considerable effort has been devoted recently to understanding the size dependence of the diffusion constant, especially the exponent α describing the power-law dependence on the [mean] radius R: $D_C = D_{co}R^{-\alpha}$. In approaching this problem we

pursued the perspective that the fluctuations of the cluster are in essence the fluctuations of its boundary, which is a closed single-height step [5, 37]. Hence, we adapted the formalism for open nearly straight steps to closed nearly circular steps. Denoting by $r(\theta,t)$ the radial distance of the edge from the center of mass, we define a normalized deviation $g(\theta,t)$ from a perfect circle and do the equivalent of capillary-wave decomposition:

$$g(\theta,t) \equiv (r(\theta,t)/R) - 1 = \sum_n g_n(t) e^{in\theta} \qquad (10)$$

The Langevin equation for $g_n(t)$ is basically the same as eqn. (2) for $x_q(t)$, with τ_n^{-1} replacing τ_q^{-1} Our previous calculations for straight steps can be carried over to circular steps by making the replacement $q \rightarrow n/R$. Since the displacement of the center of mass at time t is given by $r_{CM}^2 = x_{CM}^2 + y_{CM}^2$, we find [5,37]

$$D_c \equiv \langle r_{CM}^2 \rangle / 4t = R^2 \langle |g_1|^2 \rangle / t = R^2 f_1 = D_\alpha R^{-\alpha}. \qquad (11)$$

(In going from linear to circular geometry, a new term appears which is proportional to g and is associated with changes in cluster size. The derivation in ref. [5] of the equivalents of eqn. (11) explicitly neglects this term, as discussed in its Appendix. When we do include it, we find that eqn. (11) is unchanged, but we must modify many intermediate steps and, in the process, gain new physical insight [38].) For the cases EC, TD, and PD, since $\tau_q^{-1} \propto f_q \propto q^2, |q|^3, q^4$, we now have $f_1 \propto R^{-2}, R^{-3}, R^{-4}$, and so $\alpha = 1, 2, 3$, respectively, or equivalently, $D_c \propto N^{-1/2}, N^{-1}, N^{-3/2}$. In passing we note that for late-stage coarsening by cluster coalescence—in contrast to the near-constant size regime treated here—Sholl and Skodje [39] show that the average cluster radius increases like t^β, where $\beta = 1/(\alpha+2) = 1/3, 1/4, 1/5$, respectively, rather than the $t^{1/3}$ behavior for all 3 cases in the limit of Ostwald ripening. Furthermore, they find the dynamic scaling law for n_s, the density of islands of area s: $n_s(t) \sim t^{-2\beta} f(s/t^{2\beta})$. Several recent experiments [40–42] have carefully examined the island coalescence on Cu and Ag; such work is described in this volume by Rosenfeld *et al.* [42].

Our analysis of cluster diffusion makes all the assumptions of the straight-step analysis plus taking the step stiffness and the relevant kinetic coefficients as isotropic. Initially it seemed that the experimental situation could be well described by this simple picture. In this framework, the Morgenstern *et al.* [43] experiment for Ag(111) single-layer pits appeared to be an example of TD, as they themselves concluded [43a] from an argument following the approach of Pimpinelli *et al.* [14]; specifically, they found that $\alpha = 1.97 \pm 0.39$ for R between 10 and 75 atomic spacings (viz. 2.9Å). Microscopically, the assumed picture was that Ag atoms cannot surmount the barrier posed by the bounding step, so that they are trapped inside the pit, prohibiting the particle fluctuations associated with EC. Subsequent evidence favored diffusion predominantly by adatom motion around the pit periphery [43c]. For Ag atoms on Ag(100) Wen *et al.* [44a] reported $1/2 \leq \alpha \leq 1$. On the other hand, Wen *et al.* [44] reported behavior that seemed consistent with EC. There were considerable particle fluctuations: Wen *et al.* [44a] remark that they exclude islands which decrease in area by more than 20% during the course of the observations. Moreover, the islands are more nearly square than circular [41,44b]; much of the evaporation may occur by an edge-peeling mechanism [45] which is rate-limited by the detachment of a corner atom and so virtually independent of island size. In that case, the experimental exponent α could be more like 1/2 than 1. However, in a subsequent experiment with more extensive statistics, Pai *et al.* [40] reported PD

behavior for Cu islands on Cu(100) and Ag islands on Ag(100), consistent in the latter case with measurements of vicinal Ag(100) [28].

To check whether this behavior, based on a continuum viewpoint, is applicable to vacancy clusters on the scale of the experiments, we performed Monte Carlo simulations using the standard Metropolis algorithm. (It is, perhaps, worth mentioning that the Metropolis—as distinguished from kinetic—Monte Carlo has served successfully in obtaining quantitative agreement between theory and experiment for surface processes [46].) Since the goal was not to replicate any experiment, we invoked several simplifications and "tricks" to bring out the central physics with minimal complications. However, we did demand consistency in the three transport coefficients associated with fluctuations of straight steps and the ones associated with the cluster diffusion constant D_c. We used a square lattice with just an (attractive) nearest-neighbor (NN) energy $-\varepsilon$. We worked at $k_BT/\varepsilon = 0.6$ (0.5 for TD), well below the roughening temperature of the corresponding SOS model but high enough so that the equilibrium shape was nearly circular. For EC, we used straightforward Glauber (atom hops to/from "reservoir") dynamics, adjusting the chemical potential to keep the number of vacancies about constant. Alternatively, after removing an atom at some random value of θ, we could simply immediately reattach it at some other random position along the periphery, avoiding the nuisance of adjusting a chemical potential for the reservoir. (In this approach it is important when scaling the Monte Carlo data to include the fact that the chance of such a move per unit increases proportional to the circumference, contributing a factor of R to $D_c(R)$.) For TD, we used Kawasaki (atom hops to [NN] vacancy) dynamics. To prevent the vacancy cluster from dissolving, we forbade vacancy diffusion from the cluster boundary into the surrounding atomic lattice. To enhance motion across the terrace, we reduced the energy of an isolated atom in the interior of the monolayer pit to ε [from 4ε]; this had the added benefit of suppressing atom-cluster formation in the pit. For PD we again used Kawasaki dynamics, but with the modification that only NNN (next nearest neighbor), not NN hops were allowed. This "trick" enhanced the probability of creation, along a straight edge, of atom–notch pairs—vacancies are explicitly excluded—and prevents diffusing atoms from being trapped in corners, allowing us to achieve asymptotic PD behavior relatively quickly. Without this trick, asymptotic behavior may be reached only for larger clusters, as discussed below. We considered clusters of size 100, 400, 1600, and 6400 vacancies [embedded in a much bigger lattice] and found from log-log plots of D vs. R the best-fit exponents $\alpha = 0.97$, 2.03, and 3.1, respectively, in excellent agreement with the predictions of the continuum theory. In response to criticism [47] that these exponents were each deduced from just four data points, we note that each set of these points were nicely collinear on the log-log plot and that they spanned a greater logarithmic range than those used in the "large" regime ($100 \le N \le 1000$) in ref. [47]; we believe that we were able to obtain exponents consistent with the asymptotic limit because we chose our kinetic scheme to avoid complications, not because we used Metropolis rather than kinetic Monte Carlo. In this way, we were able to fulfill our primary goal of characterizing the asymptotic behavior in a completely self-consistent manner. The scheme does not address the size of the physical system for which asymptotia is achieved.

Our Langevin analysis also produces exact expressions for the prefactors for the three cases: $D_{co}\pi/\Omega = k_+$, D_{su}, and $a_\perp D_{st}$, respectively. The last of these is the 2D analogue of the 3D expression derived by Gruber [48]. To check the numerical values of D_{co} obtained from the y-intercepts of the log-log plots, we also computed the diffusion constant directly by applying a weak potential gradient $\mathbf{F}$ to straight steps (or to adatoms on a flat terrace for TD) and seeking the resulting average velocity $\bar{v}$. Thence, the carrier diffusion constant can be calculated from the Einstein-Nernst relation $D = k_BT\bar{v}/|F|$. The resulting values agree to within 25% with those from the log-log plots. It is tempting to extract activation energies from the prefactors, an activity in

which we have participated [5]. While the numbers obtained are semiquantitatively sensible, the level of correspondence to the real physical numbers depends on the accuracy of the presumptions made by the investigator about the microscopic Hamiltonian and how the macroscopic parameters depend on these energies.

Again, we seek a general formalism to encompass all three cases and the crossovers between them. Most of the procedures are identical to those for straight steps. E.g., we identify a cluster-edge chemical potential of the form $\mu_s = -\Omega R^{-1}\tilde{\beta}\partial^2 g/\partial\theta^2$. For simplicity we assume an atom island, with all the atomic motion on the exterior. We define two characteristic lengths: 1) $R_{su} = D_{su}/k_+$ is the ratio of the tracer (atomic) diffusion constant of the terrace D_{su} to the kinetic coefficient. When it is large, diffusion over the terrace is much greater than attachment or detachment, so the motion is limited by the latter and so more likely to be EC than TD. 2) $R_{st} = (a_\perp D_{st}/k_+)^{1/2}$ is a similar ratio of the tracer diffusion constant along the step to the mobility. To determine the cluster diffusion constant D_c, we again need only f_1. We find

$$D_c = \frac{\Omega k_+}{\pi R}\left[1+\frac{(R/R_{st})^2}{1+(R/R_{st})(R_{su}/R_{st})}\right]^{-1}. \qquad (12)$$

From eqn. (12) it is straightforward to compute the exponent $\alpha_{eff} = -\partial \log D_c/\partial \log R$ that one extracts from log-log plots of data. Fig. 4 displays this effective exponent in terms of two dimensionless ratios of the three lengths. For very small clusters, EC eventually dominates (although the continuum approximation may well fail before this limit is reached). For very large clusters (perhaps unphysically large, depending on the size of R_{su} and R_{st}, TD eventually is reached. The most important feature is that the crossover regimes are relatively narrow, little over a decade in R. This suggests that α_{eff} should attain a constant value if the data contains a large range of sizes and that one should not find values of α_{eff} other than 1, 2, or 3 for this constant. Contrary findings indicate either problems with the experiment or significant physics missing from the theoretical analysis (e.g. the edge-peeling of islands or strong anisotropy).

Some clarification of the names of the three regimes should be made. In the extreme case $D_{su} = 0$, so $R_{su} = 0$, eqn. (11) reduces to $D_c^{-1} \propto R[1 + (R/R_{st})^2]$, and we find smooth crossover directly from $\alpha = 3$ to $\alpha = 1$, as suggested by the bottom of Fig. 4. (Cf. Fig. 1b.) In this limit, atoms cannot escape from the step to the terrace, even if they can detach. Physically, when the atomic motion along the periphery is very long range, the local mass flow is effectively driven by

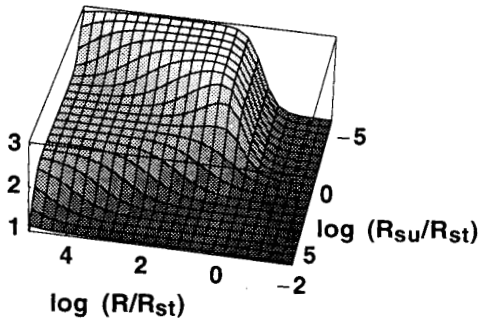

Fig. 4. 3D replot of the contour plot (Fig. 3 of ref. [5]) of the effective exponent α_{eff} as a function of the common logarithms of the dimensionless ratios R/R_{st} and R_{su}/R_{st}. The large plateaux represent $\alpha = 1$, 2, and 3, indicative of EC, TD, and PD, respectively. The crossover regions are relatively narrow.

the curvature rather than its second derivative, and we find EC-like behavior. Thus, EC denotes only that attachment/detachment limits the rate, and not that there is a finite carrier concentration on the terrace. What we label TD was called "correlated EC" by Soler [49] and by Van Siclen [45a]. The essential physical mechanism characterizing this regime is evolution by single-atom jumps from one site on the island edge to another, mediated by a concentration field on the nearby terrace region.

Kürpick *et al.* [50] showed recently via molecular dynamics, using the semiempirical EAM potential, that for vacancy islands on Ag(111) atom motion occurs predominantly by periphery mechanisms. In fact, the problem has a remarkable history. As noted above, over three decades ago, Gruber [67] found power-law scaling of $D_c(R)$ for cluster motion via PD in 3D. Almost two decades ago, Binder and Kalos [51], in studying phase separation and the consequent motion of clusters of increasing size near the critical point, argued that the diffusion constant of a cluster should decrease as an inverse power of size. Their results for cluster diffusion in a square lattice gas are of particular relevance. Almost a quarter century ago, Binder and Stauffer [52] suggested that at low temperatures dynamics are dominated by processes involving no changes in energy, viz. PD. Arguing that the number of sites $\propto R$ and the center of mass moves by R^{-2}, they deduced that the diffusivity should go like $R(R^{-2})^2$, implying $\alpha = 3$. (They also note that an evaporation-condensation process from edge sites should behave similarly.) At higher temperature, they observe that "bubbles" moving through the cluster should produce similar motion of the center of mass, but with R^2 sites participating, leading to $\alpha = 2$ as in TD. They note that for large R the motion should be dominated by processes in which some atoms evaporate into the 2-d gas while others recondense from it. In this case the displacement of the center of the cluster goes like R^{-1}, with R sites participating, leading to $\alpha = 1$ as in EC. In Monte Carlo simulations, an effective exponent close to 2 was found, which was initially attributed [53] to TD behavior. However, subsequent reconsideration [51] led to the belief—supported by simulations at $\epsilon/k_BT = 1.5$ and 2.0—that the most likely explanation is that they were seeing crossover behavior of the form

$$D_c \sim D_{co} R^{-3} [1 + R^2 \exp(-3\epsilon/k_BT)]. \qquad (13)$$

This experience provided an early warning that the size of clusters studied in current experiments and simulations with lattice-gas or semiempirical interactions may not be large enough to achieve the asymptotic regime; "corrections to [asymptotic] scaling" as in eqn. (13) may be significant. To investigate this issue thoroughly should involve the derivation of the scaling corrections from a self-consistent treatment rather than the mere *ad hoc* addition of two power-law expressions. This discussion suggests that experiments at different temperatures may be desirable or even necessary to understand the measured effective exponents. (However, there is the concomitant risk that at higher temperatures, new transport mechanisms may enter [50] that will confound the analysis!)

Metiu's group [47,54] is spearheading the systematic kinetic Monte Carlo simulation of cluster diffusion as a function of temperature as well as size. For islands on Ag(100) and on Ag(111), they [54a] find that α increases monotonically from room temperature to around 1000 K, starting at a value around or below 2 and reaching a value close to 3; for higher temperatures α decreases somewhat. Similar behavior is found [47] for model systems with plausible energy barriers. Note that in crossover of the form predicted by eqn. (13), the value of α should *decrease* as temperature increases, as occurs in these simulations at high temperature. The lower-temperature behavior is reminiscent of that found by Giesen *et al.* [25] for vicinal Cu(100). Their proposed explanation—supported by analytic and Monte Carlo results—was that at lower temperatures, one was seeing primarily random adatom hopping along the edge between pinning

sites, with an effective α of 1. At higher temperature, PD continuum behavior began to emerge. Similar observations were made for vicinal Au(110) [21] and vicinal Ag(100)[28].

It is tempting to imagine R_{st} as a sort of mean effective hop length, even though strictly speaking this parameter comes out of a continuum analysis and cannot rigorously be related to microscopic properties. In the extreme case $R_{st} = a_{\|}$, we recover $\alpha = 3$ of PD. If, inspired by Blagojević and Duxbury [14], we examine a probability distribution P(y) of various hop lengths of a single atom, then this limit corresponds to a delta function: $P(y) = \delta(y - a)$. In the opposite limit P(y) = constant, the physics is reminiscent of the EC case, since the atom can return with equal probability to any site on the step or cluster edge. Hence, $\alpha = 1$. Note that it does not matter how this distribution was achieved, i.e. what—in the language of Pimpinelli *et al.* [14]—the nature or dimensionality of the "pipe" is. As the intermediate case it seems reasonable to suppose $P(y) \propto \exp(-y/\xi)$, where ξ is a characteristic length scale which should be comparable to R_{st}. If ξ (or R_{st}) is $a_{\|}$, then P(y) becomes highly peaked near $x = 0$ since $a_{\|}/R \ll 1$; this is the delta-function limit. On the other hand for $R_{st} \gg R$, P(y) is effectively constant, as in the other limit.

CLUSTER RESPONSE TO ELECTROMIGRATION

Finally, we describe briefly our current studies of the fluctuations, dynamics, and instabilities of vacancy islands during electromigration, generalizing earlier work on straight steps without driving forces [30,55]. We emphasize the dependence on the mass-transport mechanism in the three limiting cases. In particular, we find non-circular steady states and derive the out-of-equilibrium diffusion constant of the vacancy cluster. Analytical calculations are corroborated by both Monte Carlo simulations and numerical solution of the model.

Since surface electromigration is one of the most important sources of size limitation in electric devices, it is clearly important to understand how surface morphology is affected by it. Latyshev *et al.* [56] discovered that it induces step bunching of Si(111) vicinal surfaces. How electromigration affects more complex surface structures is still poorly understood. Our first step towards complexity is the study of a closed step (monolayer atom or vacancy island). Responses of these clusters to electromigration shares similarities with void behavior in metal electric lines [57]. Qualitative differences are found between the three cases. Indeed, cluster behavior at equilibrium is already known to depend on these mechanisms. We develop a Langevin formalism based on the BCF model [58] in manner similar previous recent studies for growth of vicinal surfaces [30]. Noise correlation is calculated with the help of the approximation of local thermal equilibrium.

We determine cluster drift velocity, in particular dependence on cluster size. In the three limiting cases, we find $V \sim R^{2-\alpha}$. In the EC case, non-circular drifting steady states are found to be induced by non-instantaneous attachment kinetics for vacancy clusters. They are elongated perpendicularly to the migration axis. There are noteworthy differences between the evolution of atom and vacancy clusters.

Periphery diffusion is known to induce morphological instability leading to cluster splitting [59]. We find that adatom diffusion across the terrace induces a new morphological instability for vacancy clusters and have investigated the instability threshold. The presence of an electric field may also affect attachment/detachment rates. If so, we find novel properties of cluster motion.

Out-of-equilibrium shape fluctuations and the cluster diffusion constant are studied in the framework of our Langevin model. We find evidence that diffusion across a vacancy cluster (EC or TD) induces an anisotropic response of the cluster, whereas the response for pure PD remains isotropic for weak electromigration. The behavior of fluctuations close to the instability threshold

has been explored. Our results have considerable experimental relevance: New phenomena should be observed on metal surfaces and for voids in [2D] electric ["bamboo"] lines.

CONCLUSIONS AND CLOSING COMMENTS

We have shown how capillary-wave analysis in a Langevin framework is a conceptually enlightening and calculationally fruitful way to scrutinize quantitative data now available on step fluctuations. For both isolated steps and vicinal surfaces, the problem can be treated in a unified way within a single Langevin equation. Phase space is conveniently explored in terms of the dimensionless ratios a_q, b_q, $|q|\ell$, and r. It is dominated by limiting cases characterized by distinct physical mechanisms of atomic motion, reflected in integer values of the dynamic exponent z_q. We have examined in detail these limits and the crossover between them. To see behavior associated with a perfect Schwoebel barrier requires asymmetries in the kinetic coefficients of about a million to one. The crossover between [isolated-step] terrace diffusion and step-to-step diffusion is rather insensitive to all the dimensionless ratios except $|q|\ell$. We have also proposed an alternative formalism which uses different step attachment/detachment kinetic coefficients for processes involving terraces and for those involving the step edge.

The same perspective that is used for conventional steps near equilibrium can be applied to the closed, nearly circular steps defining a monolayer island. As a continuum approximation, this approach should break down by the atomistic level. To supplement the asymptotic behavior we have studied, corrections to scaling should be studied, as should asymmetries in the stiffness, to account for recent experimental data, which suggest physically rich behavior.

Our philosophy is to work at the continuum, macroscopic level using the step stiffness and transport coefficients as principal parameters. Monte Carlo simulations are used to check analytical predictions. In simple microscopic models, one can compute the values of these coarse-scale parameters as a check of consistency. However, it is risky to do the reverse—to deduce microscopic energies, barriers, and hopping frequencies from macroscopic data—since physical systems tend to be quite complicated, making the extracted *effective* energies different from actual physical ones. Instead, the most meaningful test of our procedure is whether the deduced macroscopic parameters provide a consistent framework for describing a broad range of observable, non-microscopic processes: step fluctuations near equilibrium, island/cluster diffusion, step bunching or unbunching, out-of-equilibrium, externally-driven motion (e.g. electromigration). The Monte Carlo calculations we perform are to check the consistency of the macroscopic parameters and to verify analytic predictions rather than to deduce rates. Thus, there is no drawback to our using Metropolis rather than kinetic Monte Carlo in our simulations.

ACKNOWLEDGMENTS

This work was supported by NSF MRSEC grant DMR-96-32521. TLE also benefited from a Humboldt U.S. Senior Scientist Award and the hospitality of the IGV/KFA Jülich. SVK thanks the Department of Energy –Basic Energy Sciences, Division of Materials Sciences for support of his work at Ohio State University. We gratefully acknowledge extensive collaboration with N.C. Bartelt, as well as ongoing collaboration helpful discussions with E.D. Williams and J.E. Reutt-Robey and their experimental groups, and helpful conversations with D.-J. Liu and S. Kodiyalam.

REFERENCES

1. N. C. Bartelt, T. L., Einstein, and E. D. Williams, Surface Sci. **273**, 252 (1993).
2. N. C. Bartelt, T. L., Einstein, and E. D. Williams, Surface Sci. **312**, 411 (1994).
3. T. L. Einstein and S. V. Khare, in Dynamics of Crystal Surface and Interfaces, P. M. Duxbury and T. J. Pence, eds. (Plenum,New York, 1997), 83.
4. S. V. Khare and T. L. Einstein, Phys. Rev. B **57**, 4782 (1998).
5. S. V. Khare and T. L. Einstein, Phys. Rev. B **54**, 11752 (1996).
6. W. W. Mullins, J. Appl. Phys. 28, 333 (1957); J. Appl. Phys. 36, 77 (1959); in Metal Surfaces: Structure, Energetics and Kinetics, N.A. Gjostein and R.W. Roberts, eds., Am. Soc. Metals, Metals Park, Ohio, 1963), p. 17.
7. N. C. Bartelt, T. L. Einstein, and E. D. Williams, Surface Sci. **276**, 308 (1992).
8. M. Kardar, Turkish J. of Phys. **18**, 221 (1994).
9. N. C. Bartelt, J. L. Goldberg, T. L. Einstein, and E. D. Williams, Surface Sci. **273**, 252 (1992).
10. N. C. Bartelt, J. L. Goldberg, T. L. Einstein, E. D. Williams, J. C. Heyraud, and J. J. Métois, Phys. Rev. B **48**, 15453 (1993).
11. N. C. Bartelt and R. M. Tromp, Phys. Rev. B **54**, 11731 (1996).
12. W. W. Pai, N. C. Bartelt, and J. E. Reutt-Robey, Phys. Rev. B **53**, 15991 (1996).
13. G. S. Bales, and A. Zangwill, Phys. Rev. B **41**, 5500 (1990).
14. A. Pimpinelli, J. Villain, D. E. Wolf, J. J. Métois, J. C. Heyraud, I. Elkinani, and G. Uimin, Surface Sci. **295**, 143 (1993).
15. B. Blagojević and P. M. Duxbury, in Dynamics of Crystal Surface and Interfaces, P. M. Duxbury and T. J. Pence, eds (Plenum, New York, 1997), 1.
16. J. S. Ozcomert, W. W. Pai, N. C. Bartelt, T. L. Einstein, and J. E. Reutt-Robey, J. Vac. Sci. Technol. A **12**, 2224 (1994).
17. J. E. Reutt-Robey and W. W. Pai, in Surface Diffusion: Atomistic and Collective Processes, M. C. Tringides, ed., NATO-ASI Series B, vol. **360** (Plenum, New York, 1997), p. 475.
18. C. Alfonso, J. M. Bermond, J. C. Heyraud, and J. J. Métois, Surface Sci. **262**, 37 (1992).
19. N. C. Bartelt, R. M. Tromp, and E. D. Williams, Phys. Rev. Lett. **73**, 1656 (1994).
20. L. Kuipers, M. S. Hoogeman, and J. W. M. Frenken, Phys. Rev. Lett. **71**, 3517 (1993).
21. L. Kuipers, M. S. Hoogeman, J. W. M. Frenken, and H. van Beijeren, Phys. Rev. B **52**, 11387 (1995).
22. M. Poensgen, J. F. Wolf, J. Frohn, M. Giesen, and H. Ibach, Surface Sci. **274**, 430 (1992).
23. M. Giesen-Seibert, R. Jentjens, M. Poensgen, and H. Ibach, Phys. Rev. Lett. **71**, 3521 (1992); **73**, E911 (1994).
24. M. Giesen-Seibert and H. Ibach, Surface Sci. **316**, 205 (1994)
25. M. Giesen-Seibert, F. Schmitz, R. Jentjens, and H. Ibach, Surface Sci. **329**, 47 (1995).
26. a) L. Masson, L. Barbier, J. Cousty, and B. Salanon, Surface Sci. **317**, L1115 (1994); b) L. Barbier, L. Masson, J. Cousty, and B. Salanon, Surface Sci. **345**, 197 (1996).
27. M. S. Hoogeman, D. C. Schlosser, and J. W. M. Frenken, Phys. Rev. B **53**, R13299 (1996).
28. P. Wang, H. Pfnür, S. V. Khare, T. L. Einstein, E. D. Williams, W. W. Pai, and J. E. Reutt-Robey, Bull. Am. Phys. Soc. **41**, 189 (1996), and preprint.
29. M. Giesen, G. Schulze Icking-Konert, H. Ibach, Surface Sci. **366**, 229 (1996).
30. O. Pierre-Louis and C. Misbah, Phys. Rev. B **58**, xxx (1998).
31. O. Pierre-Louis, Ph. D. thesis, University of Grenoble 1.
32. G. S. Bales and A. Zangwill, Phys. Rev. B **41**, 5500 (1990).
33. T. Ihle, C. Misbah, and O. Pierre-Louis, Phys. Rev. B **58**, xxx (1998).
34. H. Bonzel and W. W. Mullins, Surface Sci. **350**, 285 (1996).
35. S. V. Khare, Ph. D. thesis, University of Maryland, College Park.

36. A. Bogicevic, Ph.D. dissertation, Chalmers University of Technology, Gothenberg, Sweden, 1998; A. Bogicevic, J. Strömquist, and B.I. Lundqvist, submitted for publication.
37. S. V. Khare, N. C. Bartelt, and T. L. Einstein, Phys. Rev. Lett. **75**, 2148 (1995).
38. For example, in the equilibrium equipartition equation [P. Nozières in Solids Far From Equilibrium, C. Godrèche, ed. (Cambridge Univ. Press, Cambridge, 1992), chap. 1] $\langle |g_n(t)|^2 \rangle = k_B T/2\pi R\beta n^2$, n^2 is replace by n^2-1. Thus, the n=1 mode associated with diffusion appears to diverge. The interpretation is that $\langle |g_n(t)|^2 \rangle$ and τ_1 become proportional to time; the early-time arguments near eqn. (20) of ref. [5] are no longer needed. Physically, the n=1 mode of clusters corresponds to the q=0 mode of [isolated] steps in that displacements cost no energy.
39. D. S. Sholl and R. T. Skodje, Physica A **231**, 631 (1996).
40. W. W. Pai, A. K. Swan, Z. Zhang, and J. F. Wendelken, Phys. Rev. Lett. **79**, 3210 (1997).
41. L. Bardotti, M. C. Bartelt, C. J. Jenks, C. R. Stoldt, J.-M. Wen, C.-M. Zhang, P. A. Thiel, and J. W. Evans, Langmuir, **14**, 1487 (1998).
42. G. Rosenfeld, M. Esser, K. Morgenstern, and G. Comsa, this MRS proceedings volume.
43. a) K. Morgenstern, G. Rosenfeld, B. Poelsema, and G. Comsa, Phys. Rev. Lett. **74**, 2058 (1995); b) K. Morgenstern, G. Rosenfeld, and G. Comsa, Phys. Rev. Lett. **76**, 2113 (1996); c) G. Rosenfeld, K. Morgenstern, and G. Comsa, in Surface Diffusion: Atomistic and Collective Processes, M. C. Tringides, ed., NATO-ASI Series B, vol. **360** (Plenum, New York, 1997), p. 361.
44. a) J. M. Wen, S.-L. Chang, J. W. Burnett, J. W. Evans, and P. A. Thiel, Phys. Rev. Lett. **73**, 2591 (1994); b) J. M. Wen, J. W. Evans, M. C. Bartelt, J. W. Burnett, and P. A. Thiel, Phys. Rev. Lett. **76**, 652 (1996)
45. a) C. DeW. Van Siclen, Phys. Rev. Lett. **75**, 1574 (1995); b) J. W. Evans, P. A. Thiel, and R. Wang, 1997, unpublished.
46. A. K. Schmid, R. Q. Hwang, and N. C. Bartelt, Phys. Rev. Lett. **80**, 2153 (1998).
47. A. Bogicevic, S. Liu, J. Jacobsen, B. Lundqvist, and H. Metiu, Phys. Rev. B **57**, R9459 (1998).
48. E. E. Gruber, J. Appl. Phys. **38**, 243 (1967).
49. J. M. Soler, Phys. Rev. B **53**, R10540 (1996).
50. U. Kürpick, P. Kürpick, and T. S. Rahman, Surface Sci. **383**, L713 (1997).
51. K. Binder and M. H. Kalos, J. Stat. Phys. **22**, 363 (1980).
52. K. Binder and D. Stauffer, Phys. Rev. Lett. **33**, 1006 (1974); K. Binder, Phys. Rev. B **15**, 4425 (1977).
53. M. Rao, M. H. Kalos, J. L. Lebowitz, and J. Marro, Phys. Rev. B **13**, 7325 (1976).
54. a) T. R. Mattsson, private communication; G. Mills, T. R. Mattsson, and H. Metiu, unpublished, 1998; b) H. Metiu, T. R. Mattsson, and G. Mills, this MRS proceedings volume.
55. O. Pierre-Louis and C. Misbah, Phys. Rev. Lett. **76**, 4761 (1996).
56. A. V. Latyshev, A. L. Aseev, A. B. Krasilnikov, and S. I. Stenin, Surface Sci. **213**, 157 (1989).
57. P. S. Ho, J. Appl. Phys. **41**, 64 (1970).
58. W. K. Burton, N. Cabrera, and F. C. Frank, Phil. Trans. Roy. Soc. (London), Ser. A**243**, 299 (1951).
59. W. Wang and Z. Suo, J. Appl. Phys.**79**, 2394 (1996).